

# Geophysical Research Letters

## RESEARCH LETTER

10.1029/2019GL084375

### Key Points:

- Anaerobic methane oxidation exceeds sulfate reduction rates when microorganisms are subject to elevated methane concentrations
- Methane concentration changes have cascading effects on the microbially mediated cycling of carbon in sediments

### Supporting Information:

- Supporting Information S1

### Correspondence to:

S. B. Joye,  
 mjoye@uga.edu

### Citation:

Bowles, M. W., Samarkin, V. A., Hunter, K. S., Finke, N., Teske, A. P., Girguis, P. R., & Joye, S. B. (2019). Remarkable capacity for anaerobic oxidation of methane at high methane concentration. *Geophysical Research Letters*, *46*, 12,192–12,201. <https://doi.org/10.1029/2019GL084375>


Received 9 JUL 2019

Accepted 26 SEP 2019

Accepted article online 15 OCT 2019

Published online 8 NOV 2019

## Remarkable Capacity for Anaerobic Oxidation of Methane at High Methane Concentration

M.W. Bowles<sup>1,2</sup>, V.A. Samarkin<sup>1,3</sup>, K.S. Hunter<sup>1</sup>, N. Finke<sup>1,4</sup>, A.P. Teske<sup>5</sup>, P.R. Girguis<sup>6</sup>, and S.B. Joye<sup>1</sup> 

<sup>1</sup>Department of Marine Sciences, University of Georgia, Athens, GA, USA, <sup>2</sup>Now at Louisiana Universities Marine Consortium, Chauvin, LA, USA, <sup>3</sup>Deceased 14 February 2017, <sup>4</sup>Department of Earth, Ocean and Atmospheric Sciences, Now at University of British Columbia, Vancouver, British Columbia, Canada, <sup>5</sup>Department of Marine Sciences, University of North Carolina, Chapel Hill, NC, USA, <sup>6</sup>Biological Labs, Harvard University, Cambridge, MA, USA

**Abstract** Anaerobic oxidation of methane (AOM), a central process in the carbon cycle of anoxic environments, moderates the release of methane from soils and sediments to water bodies and, ultimately, the atmosphere. The regulation of AOM in the environment remains poorly constrained. Here we quantified AOM and sulfate reduction (SR) rates in diverse deep seafloor samples at in situ pressure and methane concentration and discovered that, in some cases, AOM exceeded SR rates by more than four times when methane concentrations were above 5 mM. Methane concentration also affected other carbon-cycling processes (e.g., carbon assimilation) in addition to SR. These results illustrate that substantial amounts of methane may be oxidized independent of SR under in situ conditions, reshaping our view of the capacity and mechanism of AOM in methane-rich environments, including the deep biosphere, where sulfate availability is considered to limit AOM.

**Plain Language Summary** At the high pressures that typify deep ocean sediment environments (approximately 10-bar hydrostatic pressure for every 100 m in water depth), greater amounts of methane, and other gases, are dissolved in seawater and in sedimentary pore water compared to concentrations observed at sea level. Microbially mediated reactions that are influenced by methane concentration are thus quite sensitive to the methane concentration utilized in an experimental design. When deep sea sediments were subjected to more realistic methane concentration during high-pressure incubations, rates of microbial processes that cycle carbon, particularly methane oxidation, increased. These patterns were not discovered previously because incubations at pressure were not performed routinely. The data reshape our understanding of methane dynamics in marine sediments.

## 1. Introduction

Methane production in marine sediments and its subsequent migration upward through fault networks generate a variety of seafloor habitats characterized by high methane flux, including gas-rich sediments, gas hydrate mounds, and/or gas-charged brine flows (Joye et al., 2010). Biological consumption of methane in deep-sea habitats makes them a globally significant methane sink (Hinrichs & Boetius, 2002; Bowles, Samarkin, Bowles, et al., 2011). Robust data describing the magnitude and regulation of methane sinks at the seabed are essential for developing realistic models of the global methane cycle, as well as the general carbon cycle for seafloor and deep biosphere environments. Ideally microbial activity must be quantified under appropriate in situ or quasi in situ conditions (Bowles, Samarkin, & Joye, 2011).

In deep-sea samples, rates of microbial processes are usually evaluated in rate assays performed at atmospheric pressure (~1 bar; Treude et al., 2003; Joye et al., 2004), a deviation from in situ conditions that can result in substantial artifacts (de Angelis et al., 1991; Kallmeyer & Boetius, 2004). The methane concentration at saturation at 1 bar (~1.3 mM) is significantly lower than the potential concentration at 500 m (>50 mM; Duan & Mao, 2006). However, surprisingly few studies have evaluated the impact of methane concentration on the suite of potentially sensitive microbial processes that cycle this key atmospheric trace gas (Bowles, Samarkin, & Joye, 2011; Nauhaus et al., 2002; Nauhaus et al., 2007).

In marine sediments, the anaerobic oxidation of methane (AOM) is often quantitatively linked to sulfate reduction (SR) through syntrophic cooperation of archaeal and bacterial partners (Boetius et al., 2000;

Hinrichs et al., 1999; Orphan et al., 2001). However, archaeal mediation of both AOM and SR has been reported (Milucka et al., 2012), and in anoxic marine sediments, sulfate is not the only oxidant for methane. Direct interspecies electron transfer between methane-oxidizing and sulfate-reducing bacteria via intracellular nanowires is an important conduit for electron flow (McGlynn et al., 2015; Wegener et al., 2015). Similarly, anoxic marine sediments are laden with conductive minerals, such as magnetite and pyrite, that could facilitate electron transfer (Kato et al., 2012). Studies of AOM in marine (Beal et al., 2009) and freshwater (Ettwig et al., 2010; Haroon et al., 2013; Segarra et al., 2013) sediments revealed coupling between AOM and iron oxide (Beal et al., 2009; Segarra et al., 2013), manganese oxide (Beal et al., 2009), nitrite (Ettwig et al., 2010), and nitrate (Haroon et al., 2013) reduction. In anoxic brackish waters, Saxton et al. (2016) proposed coupling of humic acid reduction and AOM. Hence, there are a wide variety of potential mechanisms to support sulfate-independent AOM in marine sediments. In this work, we systematically and directly evaluated the effects of methane concentration on AOM, SR, and other carbon-cycling processes in deep-sea sediments, for example, assimilation of methane into biomass.

## 2. Materials and Methods

### 2.1. Study Sites, Sample Collection, and Pressure Tubes

The samples described here were collected on separate cruises using remotely operated vehicles or a manned deep submergence vehicle in the fall of 2006, spring of 2009, fall of 2009, and spring of 2012. Sediment samples were stored at in situ temperature until experiments were conducted. Sediment samples were collected from cold seeps in the Gulf of Mexico (GoM; 2006, 2012) and Monterey Bay (MB; spring 2009) and a hydrothermal site in Guaymas Basin (GB; fall 2009; see supporting information Figures S1–S4 and Table S1). Cores were obtained from sediments overlain by *Beggiatoa* bacterial mats, which typically mark areas of active fluid seepage and high methane concentration (Joye et al., 2004). Sediment cores were maintained intact in polycarbonate core liners with core caps loosely emplaced on the top and the overlying water bubbled with hydrated air to ensure it did not go anoxic. Sampling details are provided in the supporting information. Sediments from GoM and GB were extremely gassy and contained visible oil. MB sediment was gassy but contained no visible oil.

Experiments were carried out under strictly anoxic conditions. The upper 9 cm of sediment was transferred to an argon-purged glass bottle that was sealed with a butyl rubber stopper. The bottle headspace was purged again with argon, and sediment was homogenized by gently inverting the contents multiple times. After homogenization, the sediment was sampled and transferred to modified Hungate tubes under argon.

The bottom of each Hungate tube was cut off, and tubes were purged with Argon. Sediment was added to the tube, and a retractable butyl rubber stopper (hereafter termed plunger) was inserted into the tube's open bottom. The stopper was mobile in the tube, thus permitting compression/expansion during subsequent pressurization/depressurization. After the stopper was added, the sediment was pushed up so that it was flush with the screw end of the tube. Each sample tube was sealed with no headspace using a butyl rubber septa and screw cap. Samples from each site were incubated at in situ pressure and temperature and over a range of methane concentration (1 to 50 mM). For more details, see Bowles, Samarkin, and Joye (2011).

### 2.2. Methane and Radiotracer Amendment

After samples were transferred to the modified Hungate tubes, samples were amended with methane. Using the ideal gas law, the salinity of the pore water and the temperature of the incubation, the volume of 100% ultrahigh-purity methane required to achieve the desired dissolved methane concentration was calculated. The necessary aliquot of pure methane was added to the vial using a glass syringe and needle while the retractable plunger was gently pulled to quantitatively transfer the gas in the syringe into the modified Hungate tube, creating a methane headspace. Parallel sediment samples for methane concentration determination were collected prior to the amendment to account for methane present in the sample prior to methane addition. Final concentrations for each treatment accounted for initial and added methane concentration (see Bowles, Samarkin, & Joye, 2011, and the supporting information for details of  $^{14}\text{CH}_4$  and  $^{35}\text{SO}_4^-$  radiotracer incubations).

### 2.3. Carbon Assimilation Experiments

We estimated assimilation of carbon from bicarbonate and methane into biomass by tracking formation of particulate organic carbon (POC) from radioactive bicarbonate and methane in subsamples from the methanogenesis (MOG) and AOM incubations, respectively. After radioactive methane was purged from the MOG sample, samples were transferred into 50-ml centrifuge tubes and acidified (pH ~1) by adding 5 ml of 50% (v/v) phosphoric acid. The sample was shaken vigorously and purged with compressed air for 1 hr to remove the  $^{14}\text{CO}_2$  evolved from the tracer,  $\text{H}^{14}\text{CO}_3^-$ . Following purging, the sample was homogenized and a subsample (200  $\mu\text{l}$ ) was removed from the centrifuge tube. The subsample was transferred to a 20-ml scintillation vial, scintillation cocktail was added, and the sample counted. The disintegrations per minute (DPM) of tracer activity measured in this aliquot represented labeled bicarbonate-derived POC (e.g.,  $\text{bPO}^{14}\text{C}$ ) formed during the experiment. The bPOC formation rate was calculated from equation (4):

$$\text{bPOC} = [\text{DIC}] \times (\text{bPO}^{14}\text{C}_{\text{live sample}} - \text{bPO}^{14}\text{C}_{\text{control}} / \text{H}^{14}\text{CO}_3^-) \times 1/t \quad (1)$$

where bPOC is the bPOC formation rate ( $\text{nmol} \cdot \text{cm}^{-3} \cdot \text{day}^{-1}$ ), [DIC] is the concentration of dissolved inorganic carbon ( $\text{nmol}/\text{cm}^3$  wet sediment),  $\text{bPO}^{14}\text{C}_{\text{live sample}}$  is the activity (DPM) measured in the live sample,  $\text{bPO}^{14}\text{C}_{\text{control}}$  is the activity (DPM) measured in the killed control,  $\text{H}^{14}\text{CO}_3^-$  is the activity (DPM) of bicarbonate initially injected, and  $t$  is the incubation time (day). Isotopic discrimination ( $\alpha$ ) for the process of POC formation from bicarbonate is not known.

The rate of POC formation from methane, hereafter mPOC, was determined similarly. After AOM samples were transferred to 50-ml centrifuge tubes, they were shaken, and a 1-ml aliquot was removed and dispensed into a 20-ml scintillation vial. Next, 100  $\mu\text{l}$  of 50% (v/v) phosphoric acid was added to the sample and then mixed vigorously. The sample was vented for 24 hr to remove the  $^{14}\text{CO}_2$  evolved during AOM. Then, samples were neutralized with ~200  $\mu\text{l}$  of 9 N NaOH to pH of approximately 7. To improve counting efficiency, 500  $\mu\text{l}$  of methanol was added, and the sample was then counted on a liquid scintillation counter. The DPM determined from this subsample represents the methane-supported POC, for example,  $\text{mPO}^{14}\text{C}$ , generated during the experiment. The mPOC formation rate was estimated via equation (5):

$$\text{mPOC} = [\text{CH}_4] \times (\text{mPO}^{14}\text{C}_{\text{live sample}} - \text{mPO}^{14}\text{C}_{\text{control}} / ^{14}\text{CH}_4) \times 1/t \quad (2)$$

where mPOC is the mPOC formation rate ( $\text{nmol} \cdot \text{cm}^{-3} \cdot \text{day}^{-1}$ ),  $[\text{CH}_4]$  is the concentration of methane ( $\text{nmol}/\text{cm}^3$  wet sediment),  $\text{mPO}^{14}\text{C}_{\text{live sample}}$  is the activity (DPM) of the live sample,  $\text{mPO}^{14}\text{C}_{\text{control}}$  is the activity (DPM) of the control sample,  $^{14}\text{CH}_4$  is the activity (DPM) of the methane that was initially injected, and  $t$  is the incubation time (day). As for bPOC formation, no isotopic discrimination term ( $\alpha$ ) was included in the calculation because this factor is unknown for mPOC.

### 2.4. Geochemistry and Microbial Community Assessment

We determined concentrations of  $\text{CH}_4$ ,  $\text{SO}_4^{2-}$ , and DIC in sediment pore fluids to assess initial conditions in the samples. Methane concentrations were determined in wet sediment subsamples, while a 10-ml sediment sample was centrifuged to collect interstitial water for sulfate and DIC analysis. Sulfate concentrations were determined on an ion chromatograph as previously described (Joye et al., 2004). Methane and DIC concentrations were determined using a gas chromatograph equipped with a flame ionization detector (GC-FID). Methane sample collection and treatment was carried out as previously described (Joye et al., 2004). Methane concentrations were determined for the sediment prior to the application of additional methane gas (between 0.05 and 2 ml depending on the target concentration), so that the total methane concentration could be calculated. The concentration of DIC was determined by acidification of porewater to pH ~1 in a headspace vial,  $\text{CO}_2$  was quantitatively converted into methane by a nickel catalyst, and the methane was measured by a GC-FID (Bowles, Samarkin, & Joye, 2011). For phylogenetic microbial community characterization, published 16S rRNA gene sequences were selected that represent the widely occurring methane-oxidizing archaea [ANME-1, ANME-2a-d] found in methane-rich GB, GoM, and MB sediments.

### 2.5. Paired Radiotracer and Concentration Change Over Time Experiment

We also estimated rates of SR fueled by AOM versus endogenous organic carbon by quantifying concentration changes in sulfate concentration in triplicate subsamples that were incubated with or without a

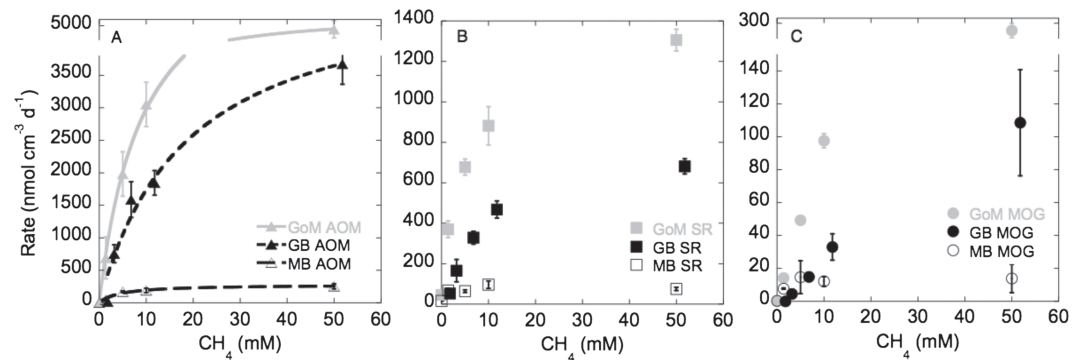


**Figure 1.** Radiotracer-derived rates of (a) anaerobic oxidation of methane (AOM), (b) sulfate reduction (SR), and (c) methanogenesis (MOG) in  $\text{nmol}\cdot\text{cm}^{-3}\cdot\text{day}^{-1}$  versus methane concentration (mM) in Gulf of Mexico (GoM), Guaymas Basin (GB), and Monterey Bay (MB) sediments at in situ pressure and temperature. Error bars represent the standard deviation of the mean ( $n = 3$ ).

methane-enriched headspace, respectively. Radiotracer-amended samples for AOM and SR were incubated in parallel to assess the coherence of the two approaches. Samples for this experiment were collected from the GoM (MC118, location above) in 2012. Samples were incubated at in situ temperature ( $5\text{ }^{\circ}\text{C}$ ) and pressure (100 bar). Sample preparation was carried out as described in prior sections, and sediments were amended with either 20- or 50-mM methane, and replicates were incubated with and without  $\text{SO}_4^{2-}$  radiotracer at in situ pressure and temperature. To track changes in concentration, an initial sample (time 0) was collected, and another sample was collected over a time series incubation. Geochemistry samples for sulfate and dissolved inorganic carbon concentration were collected immediately after sample depressurization and analyzed as described previously. The methane-amended treatments reflected SR coupled to AOM and endogenous organic matter, while the treatments without methane allowed us to estimate the fraction of SR fueled solely by endogenous organic matter. The difference in SR between these two treatments reflects SR coupled to AOM.

### 3. Results and Discussion

#### 3.1. Impact of Methane Concentration on AOM Capacity and Coupling to SR

Hydrocarbon seeps are globally abundant, biologically diverse ecosystems. The high methane concentration typical of the seafloor seeps and vents, from  $>15$  up to  $\sim 80$  mM (Lapham et al., 2013; Wankel et al., 2010), influences rates of microbially mediated processes that are sensitive to methane concentration. We observed that rates of SR, AOM, MOG, and carbon assimilation into biomass differed remarkably in incubations with high ( $>5$  mM) versus low ( $\sim 1$  mM) methane concentration (Figure 1). Increased pressure alone in the presence of 10-mM methane did not affect AOM or SR rates or coupling between the two processes (Figure S5), underscoring the central role of methane availability, as opposed to pressure, in driving the observed patterns of carbon dynamics.

Rates of AOM displayed a Michaelis-Menten-like response to methane concentration. Maximum rates of AOM in GoM and GB sediments (at  $4,800 \pm 400$  and  $3,600 \pm 300$   $\text{nmol}\cdot\text{cm}^{-3}\cdot\text{day}^{-1}$ , respectively) are among the highest activity documented directly measured using radiotracers (Figure 1a). The estimated apparent  $V_{\text{max}}$  for AOM in GoM and GB oily, gassy sediment was  $5,700 \pm 200$  and  $5,000 \pm 1,200$   $\text{nmol}\cdot\text{cm}^{-3}\cdot\text{day}^{-1}$ , respectively (Figure 1a and the supporting information). The apparent  $V_{\text{max}}$  of AOM in gassy MB sediments,  $280 \pm 40$   $\text{nmol}\cdot\text{cm}^{-3}\cdot\text{day}^{-1}$ , was substantially lower (Figure 1a). The estimated apparent half-saturation constant ( $K_s$ ) for these anaerobic methanotrophs ranged from 4- to 18-mM methane, which exceeds significantly the saturated concentration of methane in seawater at 1 bar ( $\sim 1.5$  mM).

Rates of SR and MOG also exhibited a kinetic response to methane concentration in GoM and GB sediments (Figures 1b and 1c). Maximal SR rates in GoM and GB sediments were  $1,300 \pm 50$  and  $680 \pm 40$   $\text{nmol}\cdot\text{cm}^{-3}\cdot\text{day}^{-1}$ , respectively, and the apparent  $V_{\text{max}}$  values for SR were  $1,400 \pm 130$  and  $850 \pm 140$   $\text{nmol}\cdot\text{cm}^{-3}\cdot\text{day}^{-1}$ , respectively. SR rates were consistently lower than AOM rates at methane

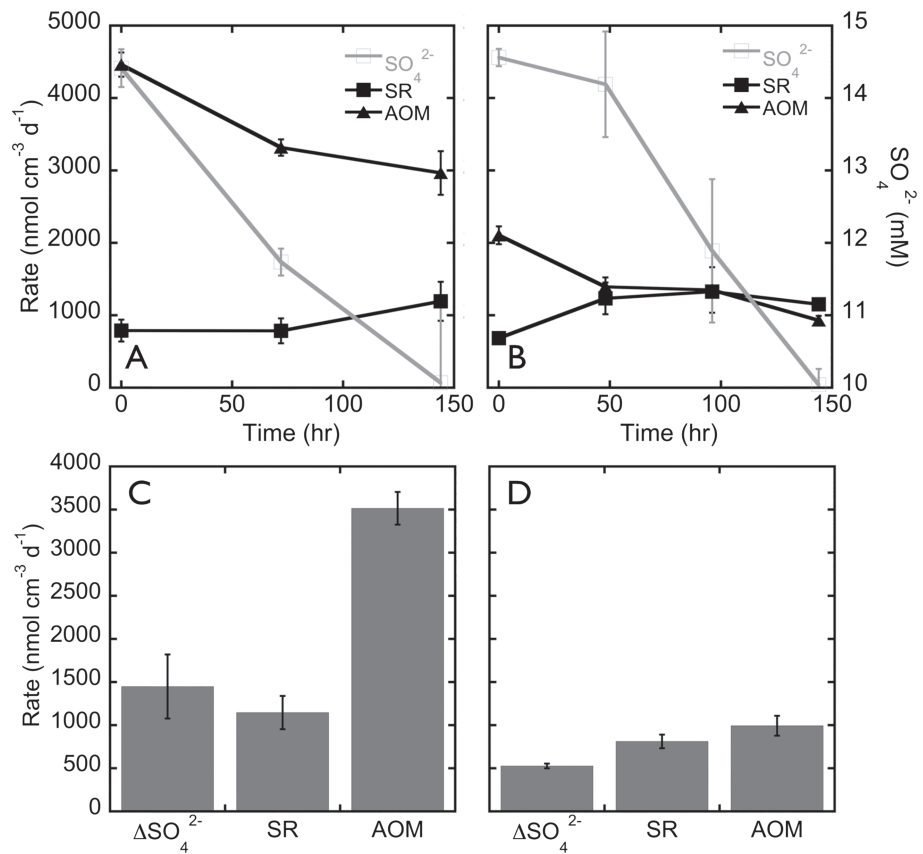


**Figure 2.** Rates of anaerobic oxidation of methane (AOM) and sulfate reduction (SR) determined in radiotracer experiments with (a) 50- and (b) 20-mM CH<sub>4</sub> as well as with the change in sulfate concentration of SO<sub>4</sub><sup>2-</sup> over time in parallel concentration change experiments. Bar graph summaries of rates from concentration change and in parallel radiotracer experiments at (c) 50 and (d) 20 mM.

concentrations above 5 mM (Figures 1a and 1b). In MB sediments, SR rates were significantly lower than those observed in GoM and GB (max: 96 nmol·cm<sup>-3</sup>·day<sup>-1</sup>) and were insensitive to methane concentration, though they were lower than AOM rates.

### 3.2. Decoupling AOM and SR in Experiments Without Radiotracers

In the radiotracer-free samples, changes in the concentration of sulfate over time in samples with or without added methane were used to estimate rates of SR. As observed in the other experiments, AOM rates exceeded SR rates substantially (Figure 2). The SR rate determined from the change in sulfate concentration over time was comparable to those determined in parallel <sup>35</sup>SO<sub>4</sub><sup>2-</sup> radiotracer assays. The higher methane concentration (50 mM; see Figures 2a and 2c) had a pronounced stimulatory effect on rates of AOM, but not SR, and the elevated AOM activity was sustained over several days. In contrast, AOM rates in the 20-mM methane treatment initially exceeded SR, but activity decreased over time, becoming similar to SR rates (Figures 2b and 2d); this pattern may have resulted from methane concentration dropping below the *K<sub>m</sub>* of the methanotrophs.

These data validate the other experimental results, illustrating that AOM and SR can be decoupled at high methane concentration, and underscore the possibility for remarkably high AOM rates at high methane concentration. This pattern points to the fact that some components of the methanotrophic microbial population are able to rapidly increase activity in response to changes in methane availability. Such community-level metabolic flexibility could be an adaptation to the fluctuating geochemical conditions that typify deep-sea methane-rich cold seeps (Lapham et al., 2008). It is unclear at this time, however, whether a single organism expresses either high- or low-affinity enzyme systems in response to changing methane concentrations or

whether co-occurring methanotrophs are adapted to either “high” or “low” concentrations, with one or the other dominating as a function of the methane concentration field.

Seep sediments in GB, GoM, and MB contained the commonly observed ANME archaea, ANME-1 and ANME-2a-d (Figure S6). These organisms occur globally in methane seeps (Ruff et al., 2015); some of the activity observed here is conservatively attributed to a subset of these widely distributed ANME archaea, without invoking an unknown, novel microorganism. However, since some of the observed activity is sulfate independent, additional methanotrophs capable of coupling AOM to electron acceptors other than sulfate must also exist. The ability of methane-oxidizing communities to respond rapidly to changing methane concentration would confer a functional ecological advantage, assuring consistent consumption of methane, which presumably supports biosynthesis if not growth, irrespective of concentration. Next, we consider possibilities for electron acceptor usage and metabolic pathways that increase the metabolic flexibility of methanotrophic communities.

### 3.3. A New Perspective on Methane Cycling

The data presented here reshape our view of the methane cycle in methane-rich habitats, as most previous ex situ incubations likely captured only the activity of methanotrophs active at lower dissolved methane concentration. The observation of the community's metabolic flexibility makes it essential to quantify rates of activity under quasi in situ conditions, and over a range of methane concentrations when possible, to assure that the observed activity is representative of the native environment and that the rates can be upscaled or properly incorporated into biogeochemical models.

Previous work (Nauhaus et al., 2002) documented a fivefold increase in SR as methane concentration increased from 1 to 16 mM. Over a similar methane concentration range (1.4 to 10 mM), we observed a two-fold to threefold increase in SR rates in GOM and GB sediments. At the same time, rates of AOM increased by almost 10-fold and exceeded SR rates as long as methane concentrations were >5 mM (Figure 1). Notably, we only observed 1:1 stoichiometry between SR and AOM at the low methane concentrations typical of degassed cores incubated under ex situ conditions (Figure S7); 1:1 stoichiometry was not observed at higher methane concentration. Furthermore, experiments with an inhibitor of SR, tungstate, confirmed that AOM proceeded in the absence of SR (Figure S8). The apparent independence of AOM from SR has fundamental implications for our understanding of AOM physiology and for methane and CO<sub>2</sub> cycling in marine sediments. In GoM and GB sediments, rates of AOM, SR, MOG, and POC formation—that is, biomass formation—increased with methane concentration (Figures 1 and 3), and rates of SR ranged from 18 to 50% of AOM rates. Thus, consumption of an AOM intermediate by sulfate-reducing bacteria could only support a fraction of the observed contemporaneous AOM activity, suggesting that other electron acceptors or mechanisms fueled a substantial portion of AOM (Haroon et al., 2013, Beal et al., 2009, Ettwig et al., 2010) and requiring simultaneous activity of multiple pathways of AOM.

The potential for multiple, contemporaneous AOM pathways was not apparent in previous AOM assays at 1 bar and ex situ methane concentration because AOM rates were typically less than or equal to SR rates (Hinrichs & Boetius, 2002; Bowles, Samarkin, Bowles, et al., 2011, Joye et al., 2004, Orcutt et al., 2010, Omoregie et al., 2009). Incubation at in situ pressure, elevated methane concentration, and nonlimiting methane concentration, which previously had not been performed, was necessary to reveal this dynamic. In particular, the observed absence of a 1:1 stoichiometry between methane and SO<sub>4</sub><sup>2-</sup> consumption at in situ methane concentrations makes it impractical to use sulfate profiles as proxy for methane cycling in marine sediments and means that prior studies that estimated AOM rates from SR profiles or SR rates (Hinrichs et al., 2002), or ex situ incubations (Bowles, Samarkin, Bowles, et al., 2011, and references therein), may have underestimated AOM rates.

We propose that a significant proportion of methane in deep-sea methane-rich environments can be oxidized anaerobically with electron acceptors other than sulfate. There are a number of alternate electron acceptors (e.g., nitrate [Haroon et al., 2013], nitrite (Ettwig et al., 2010), iron oxides (Beal et al., 2009; Segarra et al., 2013; Ettwig et al., 2010), or humic redox shuttles (Saxton et al., 2016)) that could support AOM when the process is decoupled from SR. The importance or potential magnitude of these electron acceptors as an oxidant for methane in the marine environment relative to sulfate has not been fully addressed. Nitrate concentrations in surficial seep sediments are typically at least 30 μM and may support a portion of methane

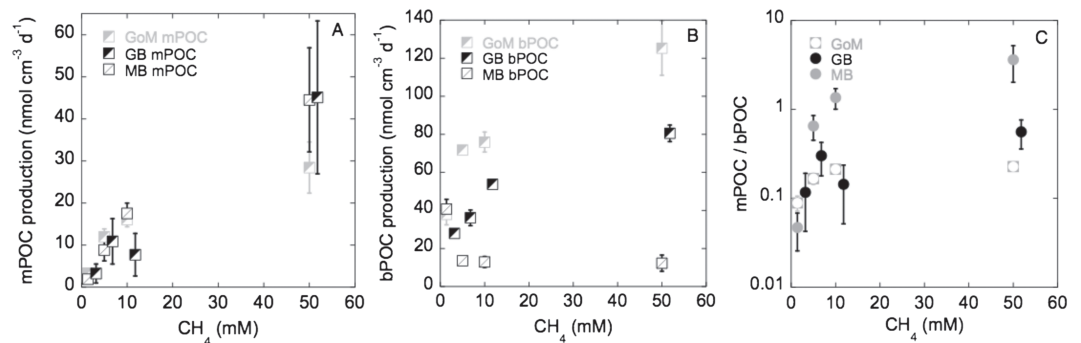


**Figure 3.** Formation rates of particulate organic carbon (POC) from each site derived from (a) methane (mPOC) and (b) bicarbonate (bPOC;  $\text{nmol}\cdot\text{cm}^{-3}\cdot\text{day}^{-1}$ ) versus methane concentration (mM). (c) Ratio of mPOC to bPOC for each site versus methane concentration (mM).

oxidation activity through coupling to denitrification (Bowles & Joye, 2011); high potential rates of denitrification ( $31 \text{ nmol}\cdot\text{cm}^{-3}\cdot\text{day}^{-1}$ ) and nitrate consumption ( $174 \text{ nmol}\cdot\text{cm}^{-3}\cdot\text{day}^{-1}$ ) were observed GB mat sediments (Bowles et al., 2012) and nitrate may be an important electron acceptor for AOM in seep and vent sediments. The large observed potential uptake rates of nitrate suggest that nitrate is likely rapidly cycled in these sediments.

Riedinger et al. (2014) hypothesized that iron reduction coupled to methane oxidation could be substantial in marine sediments where sulfate is depleted. At GoM cold seeps, solid phase Fe concentrations were highest in surficial sediments (Arvidson et al., 2004). There, the concentration of solid phase iron oxides was about  $110 \mu\text{mol/g}$ . Assuming 1 ml of sediment is  $\sim 1.4 \text{ g}$ , there would be around  $310\text{-}\mu\text{mol}$  Fe available in a 2-ml incubation. If we further assume about half of this pool is easily extractable and likely oxidized (Raiswell et al., 1994), there are  $155 \mu\text{mol}$  of oxidative capacity present in a 2-ml sample incubation. The observed maximal rate of anaerobic methane oxidation,  $5 \mu\text{mol}\cdot\text{cm}^{-3}\cdot\text{day}^{-1}$ , yields a Fe reduction rate of  $40 \mu\text{mol}\cdot\text{cm}^{-3}\cdot\text{day}^{-1}$  and a Fe-oxide turnover time of roughly 3 days assuming an 8:1 stoichiometry of Fe reduced to CH<sub>4</sub> oxidized. Manganese oxides may play a similar role (Beal et al., 2009; Segarra et al., 2013). Iron and manganese oxides are rapidly cycled in marine sediments, transitioning from oxidized to reduced states at a rapid pace (Canfield et al., 1993; Thamdrup et al., 1994). In areas of high methane flux, trace metal cycling may fluctuate between periods of accumulation and consumption, as concentrations of methane increase and decrease and metal-reducing methanotrophs modulate their activity. Notably, rapid sulfur cycling, where high rates of consumption through SR and subsequent oxidation that resupplies sulfate, is a hallmark of cold seep sediments (Lichtsschlag et al., 2010; Grunke et al., 2011; Bowles, Samarkin, Bowles, et al., 2011; Bowles, Samarkin, & Joye, 2011). Similarly rapid cycling of nitrogen and metal oxides may promote efficient consumption of methane in methane-rich habitats during periods of high methane flux.

Cold seep and hydrothermal vent environments are characterized by variable flow regimes, and individual areas may experience cycles of discharge or recharge as conduits for fluid exchange migrate (Acquolina et al., 2013). We propose that during periods of discharge when concentrations of methane in the pore fluid are high, methane is oxidized by way of a suite of electron acceptors through “metabolic phasing.” We use this term to refer to coupling of AOM to distinct electron acceptors, pending electron donor and acceptor availability. Metabolic phasing would make AOM an efficient and effective sink for methane, under fluctuating and dynamic conditions.

### 3.4. Impact of Methane Concentration on Methane Production and Carbon Assimilation

We tracked the conversion of bicarbonate to methane, that is, MOG, and observed that methane concentration stimulated methane production. Rates of methane production increased with increasing methane concentration in GoM and GB to maxima of  $265 \pm 35$  and  $108 \pm 32 \text{ nmol}\cdot\text{cm}^{-3}\cdot\text{day}^{-1}$ , respectively (Figure 1c). In MB sediments, MOG rates were lower ( $\sim 14 \text{ nmol}\cdot\text{cm}^{-3}\cdot\text{day}^{-1}$ ) and showed no relationship to methane concentration. This observed conversion of bicarbonate to methane could reflect metabolic back flux (Holler et al., 2011), but the differences between sites and lack of substantial activity at MB, despite identical incubation conditions, suggest that some portion of the activity may reflect MOG.

Methane concentration also impacted rates of carbon assimilation into microbial biomass. Patterns of biomass formation further suggest that distinct metabolic clades are involved in methane cycling. We tracked assimilation of  $^{14}\text{C}$ -labeled methane or bicarbonate into microbial biomass and observed that assimilation of methane into biomass (mPOC) was correlated positively to methane concentration. In GoM sediments, the maximum mPOC formation rate was  $29 \text{ nmol}\cdot\text{cm}^{-3}\cdot\text{day}^{-1}$  (Figure 3a). Slightly more mPOC was observed in GB and MB sediments,  $44 \text{ nmol}\cdot\text{cm}^{-3}\cdot\text{day}^{-1}$  (Figure 3b). The mPOC formation rate relative to the AOM rate was lower in GoM and GB samples (0.6% to 1.2%) compared to that in MB samples, where mPOC was up to 17% of the AOM rate (Figure 3c). The differences in mPOC formation rates relative to AOM rates between these three habitats suggest differences in anaerobic methanotroph populations, physiology, and/or methane assimilation pathway.

The rate of assimilation of bicarbonate into biomass (bPOC) almost always exceeded mPOC formation rates (Figure 3) and was positively correlated with methane concentration in GoM and GB sediments, but not in MB sediments. In GoM and GB sediments, rates of bPOC production were up to  $130 \pm 14$  and  $81 \pm 4 \text{ nmol}\cdot\text{cm}^{-3}\cdot\text{day}^{-1}$ , respectively. For MB sediments, the maximum bPOC formation rate was  $40 \pm 5 \text{ nmol}\cdot\text{cm}^{-3}\cdot\text{day}^{-1}$ . Rates of bPOC formation were typically between 1% and 10% of the AOM rate when methane concentration exceeded 5 mM (Figure 3). Collectively, bPOC and mPOC rates amounted to less than 10% of the AOM rate. At GoM and GB, bPOC production dominated, and only a small fraction of carbon assimilation was via mPOC. However, at MB, mPOC and bPOC formation rates were similar. Bicarbonate assimilation can be attributed to a number of microorganisms, including autotrophic sulfate reducers (Rabus et al., 2006) and anaerobic methanotrophs through the metabolic capacity to assimilate bicarbonate (Pernthaler et al., 2008; Kellermann et al., 2012). It is unlikely that the observed bPOC represents solely methanogenic bicarbonate assimilation since bPOC rates were comparable to or exceeded the rates of MOG (Figures 1 and 3).

The observed positive correlation between mPOC formation and methane concentration (Figure 3) documents methane assimilation by anaerobic methanotrophs at high methane concentrations. Indeed, in Black Sea microbial mats, mPOC formation was  $\sim 1.6\% \pm 0.6\%$  of the AOM rate (Treude et al., 2007) and bPOC formation amounted to approximately 10% of the AOM rate (Treude et al., 2007), as observed in AOM enrichments (Kellermann et al., 2012; Wegener et al., 2008). The mPOC and bPOC formation rates in Guaymas AOM enrichments (Kellermann et al., 2012) were similar to those documented in GoM and GB sediments (Figure 3). The present data are consistent with the idea that anaerobic methanotrophs assimilate both methane and  $\text{CO}_2$  into biomass.

Moreover, both the assimilation rate and pathway (mPOC or bPOC) were influenced by methane concentration: Anaerobic methanotrophs in MB sediments exhibited higher mPOC production rates (Figure 3), while GoM and GB anaerobic methanotrophs exhibited higher bPOC production rates (Figure 3). Interestingly, MB sediments showed a negative correlation between AOM rates and bPOC and a positive correlation between AOM rates and mPOC. These patterns suggest that different communities were involved in mPOC and bPOC dynamics in MB relative to GoM and GB.

#### 4. Conclusions

A novel method for evaluating the impact of methane concentration on rates of microbial metabolism revealed unexpected patterns of AOM relative to SR and a stimulatory effect of high methane concentration on a suite of dissimilatory and assimilatory microbial processes. Anaerobic methanotrophs used alternative, nonsulfate electron acceptors to a greater degree than previously appreciated and exhibited an unappreciated degree of flexibility through metabolic phasing, which enabled a rapid and effective response to variable methane concentration. This data set underscores the degree to which the microbial communities at deep cold seeps and vents can take advantage of varying methane concentration fields by utilizing a range of electron acceptors, thereby optimizing methane consumption. The data advance our understanding of methane dynamics and carbon cycling in the deep sea and underscore the physiological flexibility of the microbial populations inhabiting methane-rich extreme environments. By stimulating methane and DIC assimilation into biomass, AOM is interlinked with microbial production in the deep sea and shuttles methane-derived carbon widely into the benthic biosphere.



## Acknowledgments

We thank the 2009 Guaymas Basin Science party, the crew of R/V *Atlantis* and *Alvin*, S. Wankel, and Carol Lutken for assistance in acquiring samples and the Gulf of Mexico Hydrate Research Consortium for providing logistical support and ship time. This research was supported by the NOAA National Institute for Undersea Science and Technology (award numbers 06-09-018, 07-10-028, and 08-10-031), the U.S. National Science Foundation (OCE-0959337 to S. B. J. and OCE-0647633 to A. P. T.), and a grant from the Gulf of Mexico Research Initiative's "Ecosystem Impacts of Oil and Gas Inputs to the Gulf" (ECOGIG) consortium. For sampling at MC118, the Schmidt Ocean Institute's ship R/V *Falkor* was provided at no cost to facilitate access to the global ocean for researchers aligned with the Institute's vision and mission. J. Schweers assisted in the laboratory and M. Alperin, K. -U. Hinrichs, T. Hoehler, and L. Lapham provided critical comments that substantially improved previous versions of this manuscript. Data are publicly available through Gulf of Mexico Research Initiative Information & Data Cooperative at <https://data.gulfresearchinitiative.org> archived under doi:10.7266/n7-1sgh-rv35. This is ECOGIG contribution number 191.

## References

- Aquilina, A., Connelly, D. P., Copley, J. T., Green, D. R. H., Hawkes, J. A., Hepburn, L. E., et al. (2013). Geochemical and visual indicators of hydrothermal fluid flow through a sediment-hosted volcanic ridge in the Central Bransfield Basin (Antarctica). *PLoS One*, *8*, e54686. <https://doi.org/10.1371/journal.pone.0054686>
- Arvidson, R. S., Morse, J. W., & Joye, S. B. (2004). The sulfur biogeochemistry of chemosynthetic cold seep communities, Gulf of Mexico, USA. *Marine Chemistry*, *87*(3-4), 97–119. <https://doi.org/10.1016/j.marchem.2003.11.004>
- Beal, E. J., House, C. H., & Orphan, V. J. (2009). Manganese- and iron-dependent marine methane oxidation. *Science*, *325*(5937), 184–187. <https://doi.org/10.1126/science.1169984>
- Boetius, A., Ravensschlag, K., Schubert, C. J., Rickert, D., Widdel, F., Gieseke, A., et al. (2000). A marine microbial consortium apparently mediating the anaerobic oxidation of methane. *Nature*, *407*, 623–626. <https://doi.org/10.1038/35036572>
- Bowles, M. W., & Joye, S. B. (2011). High rates of denitrification and nitrate removal in cold seep sediments. *The ISME Journal*, *5*, 562–572.
- Bowles, M. W., Nigro, L. M., Teske, A. P., & Joye, S. B. (2012). Denitrification and environmental factors influencing nitrate removal in Guaymas Basin hydrothermally altered sediments. *Frontiers in Microbiology*, *3*(377). <https://doi.org/10.3389/fmicb.2012.00377>
- Bowles, M. W., Samarkin, V. A., Bowles, K. M., & Joye, S. B. (2011). Weak coupling between sulfate reduction and the anaerobic oxidation of methane in methane-rich seafloor sediments during ex situ incubation. *Geochimica et Cosmochimica Acta*, *75*(2), 500–519. <https://doi.org/10.1016/j.gca.2010.09.043>
- Bowles, M. W., Samarkin, V. A., & Joye, S. B. (2011). Improved measurement of microbial activity in deep-sea sediments at in situ pressure and methane concentration. *Limnology and Oceanography: Methods*, *9*(10), 499–506. <https://doi.org/10.4319/lom.2011.9.499>
- Canfield, D. E., Thamdrup, B., & Hansen, J. W. (1993). The anaerobic degradation of organic matter in Danish coastal sediments: Iron reduction, manganese reduction, and sulfate reduction. *Geochimica et Cosmochimica Acta*, *57*(16), 3867–3883. [https://doi.org/10.1016/0016-7037\(93\)90340-3](https://doi.org/10.1016/0016-7037(93)90340-3)
- de Angelis, M. A., Baross, J. A., & Lilley, M. D. (1991). Enhanced microbial methane oxidation in water from a deep-sea hydrothermal vent field at simulated in situ hydrostatic pressures. *Limnology and Oceanography*, *36*(3), 565–570. <https://doi.org/10.4319/lo.1991.36.3.0565>
- Duan, Z., & Mao, S. (2006). A thermodynamic model for calculating methane solubility, density and gas phase composition of methane-bearing aqueous fluids from 273 to 523 K and from 1 to 2000 bar. *Geochimica et Cosmochimica Acta*, *70*(13), 3369–3386. <https://doi.org/10.1016/j.gca.2006.03.018>
- Ettwig, K. F., Butler, M. K., Le Paslier, D., Pelletier, E., Mangenot, S., Kuypers, M. M., et al. (2010). Nitrite-driven anaerobic methane oxidation by oxygenic bacteria. *Nature*, *464*(7288), 543–548. <https://doi.org/10.1038/nature08883>
- Grünke, S., Felden, J., Lichtschlag, A., Gimth, A. C., De Beer, D., Wenzhöfer, F., & Boetius, A. (2011). Niche differentiation among mat-forming, sulfide-oxidizing bacteria at cold seeps of the Nile Deep Sea Fan (Eastern Mediterranean Sea). *Geobiology*, *9*(4), 330–348. <https://doi.org/10.1111/j.1472-4669.2011.00281.x>
- Haroon, M. F., Hu, S., Shi, Y., Imelfort, M., Keller, J., Hugenholtz, P., et al. (2013). Anaerobic oxidation of methane coupled to nitrate reduction in a novel archaeal lineage. *Nature*, *500*(7464), 567–570. <https://doi.org/10.1038/nature12375>
- Hinrichs, K. U., & Boetius, A. (2002). The anaerobic oxidation of methane: new insights in microbial ecology and biogeochemistry. In *Ocean margin systems* (pp. 457–477). Berlin, Heidelberg: Springer. [https://doi.org/10.1007/978-3-662-05127-6\\_28](https://doi.org/10.1007/978-3-662-05127-6_28)
- Hinrichs, K. U., Hayes, J. M., Sylva, S. P., Brewer, P. G., & DeLong, E. F. (1999). Methane-consuming archaeobacteria in marine sediments. *Nature*, *398*(6730), 802–805. <https://doi.org/10.1038/19751>
- Holler, T., Wegener, G., Niemann, H., Deusner, C., Ferdelman, T. G., Boetius, A., et al. (2011). Carbon and sulfur back flux during anaerobic microbial oxidation of methane and coupled sulfate reduction. *Proceedings of the National Academy of Sciences*, *108*(52), E1484–E1490. <https://doi.org/10.1073/pnas.1106032108>
- Joye, S. B., Boetius, A., Orcutt, B. N., Montoya, J. P., Schulz, H. N., Erickson, M. J., & Lugo, S. K. (2004). The anaerobic oxidation of methane and sulfate reduction in sediments from Gulf of Mexico cold seeps. *Chemical Geology*, *205*(3-4), 219–238. <https://doi.org/10.1016/j.chemgeo.2003.12.019>
- Joye, S. B., Bowles, M. W., Samarkin, V. A., Hunter, K. S., & Niemann, H. (2010). Biogeochemical signatures and microbial activity of different cold-seep habitats along the Gulf of Mexico deep slope. *Deep Sea Research Part II: Topical Studies in Oceanography*, *57*(21-23), 1990–2001. <https://doi.org/10.1016/j.dsr2.2010.06.001>
- Kallmeyer, J., & Boetius, A. (2004). Effects of temperature and pressure on sulfate reduction and anaerobic oxidation of methane in hydrothermal sediments of Guaymas Basin. *Applied and Environmental Microbiology*, *70*(2), 1231–1233. <https://doi.org/10.1128/AEM.70.2.1231-1233.2004>
- Kato, S., Hashimoto, K., & Watanabe, K. (2012). Microbial interspecies electron transfer via electric currents through conductive minerals. *PNAS*, *109*(25), 10,042–10,046. <https://doi.org/10.1073/pnas.1117592109>
- Kellermann, M. Y., Wegener, G., Elvert, M., Yoshinaga, M. Y., Lin, Y. S., Holler, T., et al. (2012). Autotrophy as a predominant mode of carbon fixation in anaerobic methane-oxidizing microbial communities. *Proceedings of the National Academy of Sciences*, *109*(47), 19,321–19,326. <https://doi.org/10.1073/pnas.1208795109>
- Lapham, L., Wilson, R., Riedel, M., Paull, C. K., & Holmes, M. E. (2013). Temporal variability of in situ methane concentrations in gas hydrate-bearing sediments near Bullseye Vent, Northern Cascadia Margin. *Geochemistry, Geophysics, Geosystems*, *14*, 2445–2459. <https://doi.org/10.1002/ggge.20167>
- Lapham, L. L., Chanton, J. P., Martens, C. S., Higley, P. D., Jannasch, H. W., & Woolsey, J. R. (2008). Measuring temporal variability in pore-fluid chemistry to assess gas hydrate stability: Development of a continuous pore-fluid array. *Environmental Science & Technology*, *42*(19), 7368–7373. <https://doi.org/10.1021/es801195m>
- Lichtschlag, A., Feldon, J., Brüchert, V., Boetius, A., & De Beer, D. (2010). Geochemical processes and chemosynthetic primary production in different thiotrophic mats of the Hakon Mosby Mud Volcano (Barents Sea). *Limnology and Oceanography*, *55*(2), 931–949. <https://doi.org/10.4319/lo.2010.55.2.0931>
- McGlynn, S. E., Chadwick, G. L., Kempes, C. P., & Orphan, V. J. (2015). Single cell activity reveals direct electron transfer in methanotrophic consortia. *Nature*, *526*(7574), 531–535. <https://doi.org/10.1038/nature15512>
- Milucka, J., Ferdelman, T. G., Polerecky, L., Franzke, D., Wegener, G., Schmid, M., et al. (2012). Zero-valent sulphur is a key intermediate in marine methane oxidation. *Nature*, *491*(7425), 541–546. <https://doi.org/10.1038/nature11656>
- Nauhaus, K., Albrecht, M., Elvert, M., Boetius, A., & Widdel, F. (2007). In vitro cell growth of marine archaeal-bacterial consortia during anaerobic oxidation of methane with sulfate. *Environmental Microbiology*, *9*(1), 187–196. <https://doi.org/10.1111/j.1462-2920.2006.01127.x>

- Nauhaus, K., Boetius, A., Krüger, M., & Widdel, F. (2002). In vitro demonstration of anaerobic oxidation of methane coupled to sulphate reduction in sediment from a marine gas hydrate area. *Environmental Microbiology*, 4(5), 296–305. <https://doi.org/10.1046/j.1462-2920.2002.00299.x>
- Omorgie, E. O., Niemann, H., Mastalerz, V., De Lange, G. J., Stadnitskaia, A., Mascle, J., & Boetius, A. (2009). Microbial methane oxidation and sulfate reduction at cold seeps of the deep Eastern Mediterranean Sea. *Marine Geology*, 261(1-4), 114–127. <https://doi.org/10.1016/j.margeo.2009.02.001>
- Orcutt, B. N., Joye, S. B., Kleindienst, S., Knittel, K., Ramette, A., Reitz, A., et al. (2010). Impact of natural oil and higher hydrocarbons on microbial diversity, distribution, and activity in Gulf of Mexico cold-seep sediments. *Deep Sea Research Part II: Topical Studies in Oceanography*, 57(21-23), 2008–2021. <https://doi.org/10.1016/j.dsr2.2010.05.014>
- Orphan, V. J., House, C. H., Hinrichs, K. U., McKeegan, K. D., & DeLong, E. F. (2001). Methane-consuming archaea revealed by directly coupled isotopic and phylogenetic analysis. *Science*, 293(5529), 484–487. <https://doi.org/10.1126/science.1061338>
- Pernthaler, A., Dekas, A. E., Brown, C. T., Goffredi, S. K., Embaye, T., & Orphan, V. J. (2008). Diverse syntrophic partnerships from deep-sea methane vents revealed by direct cell capture and metagenomics. *Proceedings of the National Academy of Sciences*, 105(19), 7052–7057. <https://doi.org/10.1073/pnas.0711303105>
- Rabus, R., Hansen, T. A., & Widdel, F. (2006). Dissimilatory sulfate- and sulfur-reducing prokaryotes. In *The prokaryotes*, (pp. 659–768). New York, NY: Springer. [https://doi.org/10.1007/0-387-30742-7\\_22](https://doi.org/10.1007/0-387-30742-7_22)
- Raiswell, R., Canfield, D. E., & Berner, R. A. (1994). A comparison of iron extraction methods for the determination of degree of pyritisation and the recognition of iron-limited pyrite formation. *Chemical Geology*, 111(1-4), 101–110. [https://doi.org/10.1016/0009-2541\(94\)90084-1](https://doi.org/10.1016/0009-2541(94)90084-1)
- Riedinger, N., Formolo, M. J., Lyons, T. W., Henkel, S., Beck, A., & Kasten, S. (2014). An inorganic geochemical argument for coupled anaerobic oxidation of methane and iron reduction in marine sediments. *Geobiology*, 12(2), 172–181. <https://doi.org/10.1111/gbi.12077>
- Ruff, E., Biddle, J. F., Teske, A., Knittel, K., Boetius, A., & Ramette, A. (2015). Global dispersion and local diversification of the methane seep microbiome. *Proceedings of the National Academy of Sciences*, 112(13), 4015–4020. <https://doi.org/10.1073/pnas.1421865112>
- Saxton, M. A., Samarkin, V. A., Schutte, C. A., Bowles, M. W., Madigan, M. T., Cadieux, S. B., & Joye, S. B. (2016). Biogeochemical and 16S rRNA gene sequence evidence supports a novel mode of anaerobic methanotrophy in permanently ice-covered Lake Fryxell, Antarctica. *Limnology and Oceanography*, 61(S1), s119–s130. <https://doi.org/10.1002/lno.10320>
- Segarra, K. E., Comerford, C., Slaughter, J., & Joye, S. B. (2013). Impact of electron acceptor availability on the anaerobic oxidation of methane in coastal freshwater and brackish wetland sediments. *Geochimica et Cosmochimica Acta*, 115, 15–30. <https://doi.org/10.1016/j.gca.2013.03.029>
- Thamdrup, B., Fossing, H., & Jørgensen, B. B. (1994). Manganese, iron and sulfur cycling in a coastal marine sediment, Aarhus Bay, Denmark. *Geochimica et Cosmochimica Acta*, 58(23), 5115–5129. [https://doi.org/10.1016/0016-7037\(94\)90298-4](https://doi.org/10.1016/0016-7037(94)90298-4)
- Treude, T., Boetius, A., Knittel, K., Wallmann, K., & Jørgensen, B. B. (2003). Anaerobic oxidation of methane above gas hydrates at Hydrate Ridge, NE Pacific Ocean. *Marine Ecology Progress Series*, 264, 1–14. <https://doi.org/10.3354/meps264001>
- Treude, T., Orphan, V., Knittel, K., Gieseke, A., House, C. H., & Boetius, A. (2007). Consumption of methane and CO<sub>2</sub> by methanotrophic microbial mats from gas seeps of the anoxic Black Sea. *Applied and Environmental Microbiology*, 73(7), 2271–2283. <https://doi.org/10.1128/AEM.02685-06>
- Wankel, S. D., Joye, S. B., Samarkin, V. A., Shah, S. R., Friederich, G., Melas-Kyriazi, J., & Girguis, P. R. (2010). New constraints on methane fluxes and rates of anaerobic methane oxidation in a Gulf of Mexico brine pool via in situ mass spectrometry. *Deep Sea Research Part II: Topical Studies in Oceanography*, 57(21-23), 2022–2029. <https://doi.org/10.1016/j.dsr2.2010.05.009>
- Wegener, G., Krukenberg, V., Riedel, D., Tegetmeyer, H. E., & Boetius, A. (2015). Intercellular wiring enables electron transfer between methanotrophic archaea and bacteria. *Nature*, 526(7574), 587–590. <https://doi.org/10.1038/nature15733>
- Wegener, G., Niemann, H., Elvert, M., Hinrichs, K. U., & Boetius, A. (2008). Assimilation of methane and inorganic carbon by microbial communities mediating the anaerobic oxidation of methane. *Environmental Microbiology*, 10(9), 2287–2298. <https://doi.org/10.1111/j.1462-2920.2008.01653.x>